This is a preprint, the final version is subject to change, of the American Mineralogist (MSA)
Cite as Authors (Year) Title. American Mineralogist, in press.
(DOI will not work until issue is live.) DOI: http://dx.doi.org/10.2138/am.2013.4219

Revision 2

Lead–tellurium oxysalts from Otto Mountain near Baker, California: IX. Agaite, $Pb_3Cu^{2+}Te^{6+}O_5(OH)_2(CO_3)$, a new mineral with CuO_5–TeO_6 polyhedral sheets.

Anthony R. Kampf[1,*], Stuart J. Mills[2], Robert M. Housley[3], and Joseph Marty[4]

[1]Mineral Sciences Department, Natural History Museum of Los Angeles County,
900 Exposition Blvd., Los Angeles, CA 90007, U.S.A.
[2]Geosciences, Museum Victoria, GPO Box 666, Melbourne 3001, Victoria, Australia
[3]Division of Geological and Planetary Sciences, California Institute of Technology, Pasadena,
CA 91125, U.S.A.
[4]5199 E. Silver Oak Road, Salt Lake City, UT 84108, U.S.A.

*e-mail: akampf@nhm.org

ABSTRACT

Agaite, $Pb_3Cu^{2+}Te^{6+}O_5(OH)_2(CO_3)$, is a new tellurate from the Aga mine on Otto Mountain near Baker, California, U.S.A. The new mineral is known from only one specimen. It occurs in vugs in quartz associated with cerussite, Br-rich chlorargyrite, chrysocolla, goethite, khinite, markcooperite, muscovite, phosphohedyphane, timroseite, and wulfenite. It is interpreted as having formed from the partial oxidation of primary sulfides and tellurides during or following brecciation of quartz veins. Agaite is orthorhombic, space group $Pca2_1$, with unit cell dimensions

a = 10.6522(7), b = 9.1630(5), c = 9.6011(7) Å, V = 937.12(11) Å^3 and Z = 4. Agaite crystals form as blades flattened on {010} and probably elongated on [001], and are up to about 20 μm thick and 200 μm in length. The color is blue, the streak is pale blue, and the luster is adamantine. The Mohs hardness is estimated at between 2 and 3. Agaite is brittle with an irregular fracture and one perfect cleavage on {010}. The calculated density based on the empirical formula is 6.987 g/cm^3. Agaite is biaxial (–), with calculated indices of refraction of α = 2.015, β = 2.065, and γ = 2.070. The measured 2V is 34(5)° and the optical orientation is X = **b**, Y = **c**, and Z = **a**. It is pleochroic: X = pale blue, Y and Z = blue; $X < Y = Z$. Electron microprobe analyses (average of 4) provided: PbO 65.91, CuO 7.75, TeO_3 17.41, CO_2 4.33 (structure), H_2O 1.78 (structure), total 97.18 wt%. The empirical formula (based on 10 O atoms *pfu*) is: $Pb_{3.00}Cu^{2+}_{0.99}Te^{6+}_{1.01}O_5(OH)_2(CO_3)$. The eight strongest powder X-ray diffraction lines are [d_{obs} in Å (*hkl*) *I*]: 4.26 (012) 28, 4.165 (211) 14, 3.303 (022, 310, 221) 100, 2.7472 (131, 203, 312) 68, 2.571 (032, 401, 231) 14, 2.0814 (332, 422) 21, 2.0306 (511) 17, and 1.7468 (multiple) 40. The crystal structure of agaite (R_1 = 0.033 for 1913 reflections with $F_o > 4\sigma F$) contains edge-sharing chains of $Cu^{2+}O_5$ square pyramids and $Te^{6+}O_6$ octahedra parallel to **a** that are joined by corner-sharing in the **c** direction, forming polyhedral sheets parallel to {010}. The polyhedral sheet is very similar to those in the structures of timroseite and paratimroseite. The thick interlayer region contains 8- and 9-coordinated Pb^{2+}, as well as CO_3 and OH groups. The Pb coordinations have lopsided distributions of bond lengths attributable to the localization of the Pb^{2+} $6s^2$ lone-pair electrons.

Keywords: Agaite; new mineral; tellurate; crystal structure; Pb^{2+} $6s^2$ lone-pair; timroseite; paratimroseite; Otto Mountain, California.

INTRODUCTION

The remarkable secondary mineral assemblage at Otto Mountain, near Baker, California, U.S.A. (Housley et al. 2011) has now yielded a total of ten new Pb–Te oxysalts: ottoite, housleyite, thorneite, markcooperite, timroseite, paratimroseite, telluroperite, chromschieffelinite, fuettererite, and agaite (see Table 1). The last of these, agaite, is described herein. Agaite is named for the type locality, the Aga mine, and for A. G. Andrews, from whose initials the name of the mine is derived. Andrews is one of two persons who are responsible for the development of the mining claims on Otto Mountain. In 1940, Otto Fuetterer filed six claims on the hill, named Good Hope 1–6. The following year, A. G. Andrews, a friend of Fuetterers, filed 18 adjacent claims named Aga 1–18; in 1942 Andrews added two more, Aga 19 and 20. The two men held these claims together until sometime after 1950 when Fuetterer became sole owner of all 26 claims.

The new mineral and name has been approved by the Commission on New Minerals, Nomenclature and Classification of the International Mineralogical Association (IMA 2011–115). One holotype specimen is deposited in the Natural History Museum of Los Angeles County, catalogue number 63590.

OCCURRENCE

The only known specimen of agaite was found by one of the authors (JM) at the Aga mine (35.27215°N, 116.09487°W, elevation 1055 feet) on Otto Mountain, 1 mile northwest of Baker, San Bernardino County, California, U.S.A. On this specimen there is only one small cluster of agaite crystals on quartz in association with cerussite, Br-rich chlorargyrite,

chrysocolla, goethite, khinite, markcooperite, muscovite, phosphohedyphane, timroseite, and wulfenite. Other species identified in the mineral assemblages at Otto Mountain include acanthite, anglesite, anatacamite, atacamite, boleite, brochantite, burckhardtite, calcite, caledonite, celestine, chalcopyrite, chromschieffelinite, clinoatacamite, devilline, diaboleite, eztlite, fluorite, fornacite, fuettererite, galena, gold, hematite, hessite, housleyite, iodargyrite, jarosite, kuranakhite, linarite, malachite, mimetite, mottramite, munakataite, murdochite, ottoite, paratimroseite, perite, plumbojarosite, pyrite, sonoraite, telluroperite, thorneite, vanadinite, and vauquelinite.

Agaite and most the other secondary minerals of the quartz veins is interpreted as having formed from the partial oxidation of primary sulfides (e.g. galena and chalcopyrite) and tellurides (e.g. hessite) during or following brecciation of the quartz veins. Additional background on the occurrence is provided in Kampf et al. (2010a) and Housley et al. (2011).

PHYSICAL AND OPTICAL PROPERTIES

Agaite occurs as blades flattened on {010} and probably elongated on [001] up to about 20 μm thick and 200 μm in length (Fig. 1). No twinning was observed optically under crossed polars or based upon single-crystal X-ray diffraction. The color is blue, the streak is pale blue, and the luster is adamantine. The Mohs hardness could not be measured, but is estimated to be between 2 and 3, based upon the behavior of crystals when broken. The new mineral is brittle with irregular fracture and one perfect cleavage on {010}. The density could not be measured because it is greater than those of available high-density liquids and there is insufficient material for physical measurement. The calculated density based on the empirical formula is 6.987 g/cm^3 and that based on the ideal formula is 6.993 g/cm^3. Insufficient material was available for

chemical tests; however, it is likely that the mineral dissolves in cold, dilute HCl with some effervescence due to the presence of CO_3.

The indices of refraction could not be measured because of the small amount of material available and the difficulty in working with liquids of sufficiently high index of refraction. We have endeavored to provide optical properties based upon a combination of measurements and calculations. Agaite is biaxial (–), with indices of refraction $\alpha = 2.015$, $\beta = 2.065$, and $\gamma = 2.070$. These were calculated from the retardation, $\gamma - \beta = 0.005$, (measured with a Berek compensator), $2V_{meas.} = 34(5)°$ (measured on a spindle stage), and $n_{av} = 2.050$ (based upon the Gladstone–Dale relationship for the ideal composition; Mandarino 2007). The dispersion could not be observed. The optical orientation is: X = **b**, Y = **c**, and Z = **a**. Agaite is pleochroic: X = pale blue, Y and Z = blue; $X < Y = Z$.

CHEMICAL COMPOSITION

Quantitative chemical analyses (4) of agaite were performed using a JEOL8200 electron microprobe (WDS mode, 15 kV, 5 nA, 1 μm beam diameter) at the Division of Geological and Planetary Sciences, California Institute of Technology. The standards used were: galena (for Pb), cuprite (for Cu), and Sb_2Te_3 (for Te). Analytical results are given in Table 2. No other elements were detected in EDS analyses. There was insufficient material for CHN analyses, so CO_2 and H_2O were calculated on the basis of 5 total cations (Pb + Cu + Te), charge balance and 10 total O atoms *pfu*, as determined by the crystal structure analysis (see below). Note that agaite is prone to electron beam damage, which contributes to the low analytical total. This is a common feature observed in most secondary tellurate species (e.g. Kampf et al. 2010a–e; Kampf et al. 2012a,b; Mills et al. 2009, 2010).

The empirical formula (based on 10 O atoms *pfu*) is: $Pb_{3.00}Cu^{2+}_{0.99}Te^{6+}_{1.01}O_5(OH)_2(CO_3)$. The simplified formula is $Pb_3Cu^{2+}Te^{6+}O_5(OH)_2(CO_3)$, which requires PbO 67.86, CuO 8.06, TeO_3 17.80, CO_2 4.46, H_2O 1.83, total 100 wt%.

X-RAY CRYSTALLOGRAPHY AND STRUCTURE DETERMINATIONS

All powder and single-crystal X-ray diffraction data were obtained on a Rigaku R-Axis Rapid II curved imaging plate microdiffractometer utilizing monochromatized Mo*K*α radiation. Observed powder *d*-values (with standard deviations) and intensities were derived by profile fitting using JADE 9.3 software. Data (in Å) are given in Table 3. Unit cell parameters refined from the powder data using JADE 9.3 with whole pattern fitting are: $a = 10.620(6)$, $b = 9.116(5)$, $c = 9.555(6)$ Å, and $V = 925.0(9)$ Å^3. The observed powder data fit well with those calculated from the structure, also using JADE 9.3. The relatively low precision of the cell refined from the powder data is attributable to the use of Mo*K*α radiation.

The Rigaku CrystalClear software package was used for processing of the diffraction data, including the application of an empirical multi-scan absorption correction using ABSCOR (Higashi 2001). The structure was solved by direct methods using SIR2004 (Burla et al. 2005). SHELXL-97 software (Sheldrick 2008) was used for the refinement of the structure. All sites were assigned full occupancy. Details concerning data collection and structure refinement are provided in Table 4. Fractional coordinates and atom displacement parameters are provided in Table 5, selected interatomic distances in Table 6 and bond valences in Table 7.

DESCRIPTION OF THE STRUCTURE

The structure of agaite (Fig. 2) contains edge-sharing chains of $Cu^{2+}O_5$ square pyramids and $Te^{6+}O_6$ octahedra parallel to **a** that are joined by corner-sharing in the **c** direction, forming polyhedral sheets parallel to {010} (Fig. 3). The $Cu^{2+}O_5$ square pyramid exhibits typical Jahn-Teller distortion, with four short equatorial bonds and one much longer apical bond. One equatorial edge is shared with a $Te^{6+}O_6$ octahedron and one equatorial–apical edge is shared with a $Te^{6+}O_6$ octahedron. The latter requires the apex of the square pyramid to be very markedly canted in the direction of the shared edge.

The thick interlayer region contains three different Pb^{2+}–O coordinations, as well as CO_3 and OH groups. The CO_3 groups are aligned approximately parallel to {010} and are located midway between the polyhedral sheets. Pb1 is 9-coordinated and both Pb2 and Pb3 are 8-coordinated. All three Pb coordinations have lopsided distributions of bond lengths attributable to the localization of the Pb^{2+} $6s^2$ lone-pair electrons (Fig. 4). The relatively weak bonding between the polyhedral sheets accounts for the perfect {010} cleavage.

The edge- and corner-sharing polyhedral sheet consisting of $Cu^{2+}O_5$ square pyramids and $Te^{6+}O_6$ octahedra in the structure of agaite is very similar to the sheets in the structures of timroseite and paratimroseite (Kampf et al. 2010e). In fact, the sheets are essentially identical if half of the Cu polyhedra in the timroseite and paratimroseite sheets are selectively removed as shown in Figure 3. Further evidence of the similarity of the sheets is provided by the cell parameters corresponding to the sheet dimensions: for agaite a = 10.6522 (2 × 5.3261) and c = 9.6011 Å; for tinmroseite a = 5.2000 and b = 9.6225 Å; and for paratimroseite a = 5.1943 and b = 9.6198 Å.

The only other known tellurate-carbonate, thorneite (Kampf et al., 2010c), is also found at Otto Mountain, but is found there at the Bird Nest drift and not at the Aga mine. As seen by its

formula, $Pb_6(Te_2O_{10})(CO_3)Cl_2(H_2O)$, thorneite contains no Cu^{2+}. Its crystal structure bears no resemblance to that of agaite and, in fact, it is the only mineral with a structure containing edge-sharing tellurate dimers.

ACKNOWLEDGEMENTS

The paper benefited from comments by reviewers Fernando Colombo and Jiří Sejkora. The Caltech EMP analyses were supported by a grant from the Northern California Mineralogical Association. The remainder of this study was funded by the John Jago Trelawney Endowment to the Mineral Sciences Department of the Natural History Museum of Los Angeles County.

REFERENCES

Burla, M.C., Caliandro, R., Camalli, M., Carrozzini, B., Cascarano, G.L., De Caro, L., Giacovazzo, C., Polidori, G., and Spagna, R. (2005) SIR2004: an improved tool for crystal structure determination and refinement. Journal of Applied Crystallography, 38, 381–388.

Brown, I.D. and Altermatt, D. (1985) Bond-valence parameters from a systematic analysis of the inorganic crystal structure database. Acta Crystallographica, B41, 244–247.

Higashi, T. (2001) *ABSCOR*. Rigaku Corporation, Tokyo, Japan.

Housley, R. M., Kampf, A. R., Mills, S. J., Marty, J., and Thorne, B. (2011) The remarkable occurrence of rare secondary tellurium minerals at Otto Mountain near Baker, California – including seven new species. Rocks and Minerals, 86, 132–142.

Kampf, A. R., Housley, R. M., Mills, S. J., Marty, J. and Thorne, B. (2010a) Lead–tellurium oxysalts from Otto Mountain near Baker, California: I. Ottoite, Pb_2TeO_5, a new mineral with chains of tellurate octahedra. American Mineralogist, 95, 1329–1336.

Kampf, A. R., Marty, J. and Thorne, B. (2010b) Lead–tellurium oxysalts from Otto Mountain near Baker, California: II. Housleyite, $Pb_6CuTe_4TeO_{18}(OH)_2$, a new mineral with Cu–Te octahedral sheets. American Mineralogist, 95, 1337–1342.

Kampf, A. R., Housley, R. M. and Marty, J. (2010c) Lead–tellurium oxysalts from Otto Mountain near Baker, California: III. Thorneite, $Pb_6(Te_2O_{10})(CO_3)Cl_2(H_2O)$, the first mineral with edge-sharing octahedral dimers. American Mineralogist, 95, 1548–1553.

Kampf, A. R., Mills, S. J., Housley, R. M., Marty, J. and Thorne, B. (2010d) Lead–tellurium oxysalts from Otto Mountain near Baker, California: IV. Markcooperite, $Pb_2(UO_2)TeO_6$, the first natural uranyl tellurate. American Mineralogist, 95, 1554–1559.

Kampf, A. R., Mills, S. J., Housley, R. M., Marty, J. and Thorne, B. (2010e) Lead–tellurium oxysalts from Otto Mountain near Baker, California: V. Timroseite, $Pb_2Cu^{2+}{}_5(Te^{6+}O_6)_2(OH)_2$, and paratimroseite, $Pb_2Cu^{2+}{}_4(Te^{6+}O_6)_2(H_2O)_2$, new minerals with edge-sharing Cu–Te octahedral chains. American Mineralogist, 95, 1560–1568.

Kampf, A. R., Mills, S. J., Housley, R. M., Marty, J. and Thorne, B. (2010f) Lead–tellurium oxysalts from Otto Mountain near Baker, California: VI. Telluroperite, $Pb_3Te^{4+}O_4Cl_2$, the Te analogue of perite and nadorite. American Mineralogist, 95, 1569–1573.

Kampf, A. R., Mills, S. J. and Housley, R. M. (2010g) The crystal structure of munakataite, $Pb_2Cu_2(Se^{4+}O_3)(SO_4)(OH)_4$, from Otto Mountain, San Bernardino County, California, USA. Mineralogical Magazine, 74, 991–998.

Kampf, A. R., Mills, S. J., Housley, R. M., Rumsey, M. S., and Spratt, J. (2012a) Lead–tellurium oxysalts from Otto Mountain near Baker, California: VII. Chromschieffelinite, $Pb_{10}Te_6O_{20}(CrO_4)(H_2O)_5$, the chromate analogue of schieffelinite. American Mineralogist, 97, 212–219.

Kampf, A. R., Mills, S. J., Housley, R. M., and Marty, J. (2012b) Lead–tellurium oxysalts from Otto Mountain near Baker, California: VIII. Fuettererite, $Pb_3Cu^{2+}{}_6Te^{6+}O_6(OH)_7Cl_5$, a new mineral with double spangolite–type sheets. American Mineralogist, 97, xxx–xxx.

Krivovichev, S. V. and Brown, I. D. (2001) Are the compressive effects of encapsulation an artifact of the bond valence parameters? Zeitschrift für Kristallographie, 216, 245–247.

Mandarino, J.A. (2007) The Gladstone–Dale compatibility of minerals and its use in selecting mineral species for further study. Canadian Mineralogist, 45, 1307–1324.

Mills, S.J., Kampf, A.R., Kolitsch, U., Housley, R.M., and Raudsepp, M. (2010) The crystal chemistry and crystal structure of kuksite, $Pb_3Zn_3Te^{6+}P_2O_{14}$, and a note on the crystal structure of yafsoanite, $(Ca,Pb)_3Zn(TeO_6)_2$. American Mineralogist, 95, 933–938.

Mills, S.J., Kolitsch, U., Miyawaki, R., Groat, L.A., and Poirier, G. (2009) Joëlbruggerite, $Pb_3Zn_3(Sb^{5+},Te^{6+})As_2O_{13}(OH,O)$, the Sb^{5+} analogue of dugganite, from the Black Pine mine, Montana. American Mineralogist, 94, 1012–1017.

Sheldrick, G. M. (2008) A short history of *SHELX*. Acta Crystallographica, A64, 112–122.

222 FIGURE CAPTIONS

223

224 Figure 1. SEM image of agaite on quartz.

225

226 Figure 2. Clinographic projection of the structure of agaite. Unit cell outline is shown as dashed
227 lines.

228

229 Figure 3. The polyhedral sheets in the structures of agaite, timroseite, and paratimroseite. The
230 sheets are essentially the same, if the unshaded CuO_5 and CuO_6 polyhedra in the sheets in
231 timroseite and paratimroseite are ignored.

232

233 Figure 4. Pb coordinations in agaite. The lopsided distributions of bond lengths are attributable to
234 the localization of the lone-pair electrons. Bond lengths are given in Å.

235

236 Table 1. New minerals described from Otto Mountain.

Mineral	Ideal Formula	Reference
Ottoite	$Pb_2Te^{6+}O_5$	Kampf et al. (2010a)
Housleyite	$Pb_6Cu^{2+}Te^{6+}_4O_{18}(OH)_2$	Kampf et al. (2010b)
Thorneite	$Pb_6(Te^{6+}_2O_{10})(CO_3)Cl_2(H_2O)$	Kampf et al. (2010c)
Markcooperite	$Pb_2(UO_2)Te^{4+}O_6$	Kampf et al. (2010d)
Timroseite	$Pb_2Cu^{2+}_5(Te^{6+}O_6)_2(OH)_2$	Kampf et al. (2010e)
Paratimroseite	$Pb_2Cu^{2+}_4(Te^{6+}O_6)_2(H_2O)_2$	Kampf et al. (2010e)
Telluroperite	$Pb_3Te^{4+}O_4Cl_2$	Kampf et al. (2010f)
Chromschieffelinite	$Pb_{10}Te^{6+}_6O_{20}(CrO_4)(H_2O)_5$	Kampf et al. (2012a)
Fuettererite	$Pb_3Cu^{2+}_6Te^{6+}O_6(OH)_7Cl_5$	Kampf et al. (2012b)
Agaite	$Pb_3Cu^{2+}Te^{6+}O_5(OH)_2(CO_3)$	This study

237

238

239 Table 2. Chemical analytical data for agaite.

Constituent	Average	Range	SD
PbO	65.91	65.43–66.61	0.55
CuO	7.75	7.60–7.98	0.17
TeO_3	17.41	17.18–17.60	0.21
CO_2*	4.33		
H_2O*	1.78		
Total	97.18		

240

241 * based on the crystal structure.

242

Table 3. X-ray powder diffraction data for agaite.

I_{obs}	d_{obs}	d_{calc}	I_{calc}	$h\ k\ l$	I_{obs}	d_{obs}	d_{calc}	I_{calc}	$h\ k\ l$
4	9.20(8)	9.1630	6	0 1 0	11	2.1308(7)	2.1262	21	0 2 4
5	5.670(7)	5.6280	7	1 1 1	21	2.0814(5)	2.0856	17	3 3 2
7	4.827(8)	4.8006	16	0 0 2			2.0760	18	4 2 2
11	4.686(10)	4.6575	8	2 0 1	17	2.0306(6)	2.0283	15	5 1 1
28	4.26(2)	4.2523	16	0 1 2			1.8938	3	5 2 1
14	4.165(7)	4.1519	38	2 1 1			1.8874	3	3 4 1
6	3.99(10)	3.9493	4	1 1 2	8	1.880(6)	1.8760	3	3 3 3
4	3.590(11)	3.5659	5	2 0 2			1.8690	4	4 2 3
11	3.485(13)	3.4733	5	2 2 0			1.8519	6	4 3 2
		3.3143	72	0 2 2			1.7583	15	2 4 3
100	3.303(2)	3.3108	27	3 1 0	40	1.7468(8)	1.7501	4	4 1 4
		3.2661	100	2 2 1			1.7411	15	5 1 3
11	3.19(10)	3.1647	4	1 2 2			1.7366	6	4 4 0
7	3.06(2)	3.0543	7	0 3 0	10	1.7174(9)	1.7191	15	5 3 1
13	2.911(5)	2.9360	5	1 3 0			1.7053	6	2 5 1
		2.9067	8	1 1 3	14	1.6810(12)	1.6805	16	2 2 5
10	2.810(3)	2.8140	4	2 2 2	8	1.6641(10)	1.6665	9	3 3 4
		2.8077	14	1 3 1			1.6616	5	4 2 4
68	2.7472(12)	2.7432	67	2 0 3	4	1.630(3)	1.6375	3	1 4 4
		2.7255	15	3 1 2			1.6285	7	3 5 0
10	2.669(6)	2.6631	15	4 0 0	3	1.602(4)	1.6070	3	1 3 5
		2.5770	7	0 3 2			1.6002	7	0 0 6
14	2.571(4)	2.5662	6	4 0 1			1.5729	7	1 5 3
		2.5541	10	2 3 1	11	1.5580(8)	1.5548	5	2 3 5
5	2.500(8)	2.5047	4	1 3 2			1.5525	4	6 0 3
11	2.327(5)	2.3287	4	4 0 2			1.4566	4	0 5 4
		2.3219	9	0 1 4	10	1.4470(8)	1.4514	3	3 5 3
7	2.296(3)	2.2908	14	0 4 0			1.4407	4	3 1 6
8	2.262(10)	2.2570	9	4 1 2	3	1.4104(4)	1.4094	4	5 1 5
5	2.1853(16)	2.1883	5	2 0 4	3	1.3710(7)	1.3716	4	4 0 6

Note: Only calculated lines with intensities greater than 5 are shown, unless they correspond to observed lines.

Table 4. Data collection and structure refinement details for agaite.

Diffractometer	Rigaku R-Axis Rapid II
X-ray radiation	Mo$K\alpha$ (λ = 0.71075 Å)
Temperature	298(2) K
Structural Formula	$Pb_3Cu^{2+}Te^{6+}O_5(OH)_2(CO_3)$
Space group	$Pca2_1$
Unit cell dimensions	a = 10.6522(7) Å
	b = 9.1630(5) Å
	c = 9.6011(7) Å
Z	4
Volume	937.12(11) Å^3
Density (for above formula)	6.993 g cm^{-3}
Absorption coefficient	59.065 mm^{-1}
F(000)	1660
Crystal size	70 × 40 × 10 μm
θ range	3.62 to 27.45°
Index ranges	$-13 \le h \le 13$, $-11 \le k \le 11$, $-12 \le l \le 12$
Reflections collected/unique	8887/2143 [R_{int} = 0.067]
Reflections with $F_o > 4\sigma F$	1913
Completeness to θ = 27.45°	99.8%
Max. and min. transmission	0.5896 and 0.1040
Refinement method	Full-matrix least-squares on F^2
Parameters refined	146
GoF	0.966
Final R indices [$F_o > 4\sigma F$]	R_1 = 0.0328, wR_2 = 0.0584
R indices (all data)	R_1 = 0.0387, wR_2 = 0.0608
Flack parameter	0.007(8)
Extinction coefficient	0.00000(5)
Largest diff. peak/hole	+2.69/–1.49 e A^{-3}

Notes: $R_{int} = \Sigma|F_o^2 - F_o^2(\text{mean})|/\Sigma[F_o^2]$. GoF = $S = \{\Sigma[w(F_o^2 - F_c^2)^2]/(n-p)\}^{1/2}$. $R_1 = \Sigma||F_o| - |F_c||/\Sigma|F_o|$. $wR_2 = \{\Sigma[w(F_o^2 - F_c^2)^2]/\Sigma[w(F_o^2)^2]\}^{1/2}$. $w = 1/[\sigma^2(F_o^2) + (aP)^2 + bP]$ where a is 0., b is 0 and P is $[2F_c^2 + \text{Max}(F_o^2, 0)]/3$.

Table 5. Fractional coordinates and atomic displacement parameters for agaite.

	x/*a*	*y*/*b*	*z*/*c*	U_{eq}	U_{11}	U_{22}	U_{33}	U_{23}	U_{13}	U_{12}
Pb1	0.38350(4)	0.73371(6)	0.57261(5)	0.01575(13)	0.0170(2)	0.0174(3)	0.0129(3)	0.0008(3)	-0.0011(3)	0.00409(18)
Pb2	0.80327(4)	0.71021(6)	0.56008(7)	0.01820(14)	0.0148(2)	0.0210(3)	0.0188(2)	0.0014(3)	0.0004(3)	-0.0020(2)
Pb3	0.61180(5)	0.03814(7)	0.42405(7)	0.02222(16)	0.0201(3)	0.0174(3)	0.0292(4)	-0.0003(3)	0.0005(3)	-0.0006(2)
Te	0.37010(7)	0.52602(11)	0.26536(10)	0.0103(2)	0.0089(4)	0.0150(5)	0.0071(4)	-0.0001(4)	-0.0003(3)	0.0009(4)
Cu	0.60759(14)	0.4391(2)	0.40337(18)	0.0128(4)	0.0105(7)	0.0187(10)	0.0093(9)	-0.0010(8)	-0.0004(6)	0.0020(7)
C	0.3597(13)	0.0182(16)	0.285(2)	0.022(4)	0.013(7)	0.015(8)	0.036(11)	-0.008(7)	-0.002(7)	0.002(6)
O1	0.3605(8)	0.0268(11)	0.4147(12)	0.027(3)	0.020(5)	0.039(7)	0.022(6)	-0.001(5)	0.011(5)	0.004(5)
O2	0.2545(10)	0.0212(11)	0.2157(12)	0.028(3)	0.022(5)	0.030(7)	0.032(7)	0.010(5)	-0.008(5)	-0.009(5)
O3	0.4655(9)	0.0042(13)	0.2140(13)	0.033(3)	0.023(6)	0.046(8)	0.029(7)	0.006(5)	0.005(5)	0.018(6)
O4	0.2538(10)	0.6677(9)	0.3293(11)	0.014(2)	0.011(4)	0.015(5)	0.016(5)	-0.005(5)	-0.004(4)	-0.004(5)
O5	0.2579(10)	0.3716(10)	0.3093(12)	0.019(2)	0.020(4)	0.030(6)	0.009(4)	0.005(5)	0.002(3)	-0.013(6)
O6	0.6933(7)	0.4803(9)	0.5782(11)	0.015(2)	0.008(4)	0.028(5)	0.008(5)	-0.002(5)	0.006(4)	0.000(4)
O7	0.5136(8)	0.4012(10)	0.2338(9)	0.0121(19)	0.015(4)	0.011(5)	0.011(5)	0.001(4)	0.000(4)	0.003(4)
O8	0.4461(8)	0.5275(10)	0.4492(10)	0.016(2)	0.013(4)	0.023(6)	0.011(5)	0.000(4)	0.000(4)	-0.001(4)
OH9	0.4810(8)	0.6911(11)	0.2088(9)	0.020(2)	0.013(5)	0.029(7)	0.018(5)	0.003(5)	0.014(4)	-0.005(4)
OH10	0.5938(7)	0.8010(12)	0.4712(10)	0.020(2)	0.007(4)	0.028(6)	0.025(6)	-0.005(5)	-0.001(4)	-0.005(4)

Note: All sites were assigned full occupancy.

Table 6. Selected bond lengths (Å) in agaite.

Pb1–O7	2.264(8)	Pb2–O6	2.417(8)	Pb3–OH10	2.228(11)
Pb1–O8	2.327(9)	Pb2–OH10	2.530(9)	Pb3–O3	2.568(12)
Pb1–OH10	2.519(9)	Pb2–O5	2.567(11)	Pb3–O2	2.570(11)
Pb1–O4	2.780(10)	Pb2–O5	2.591(11)	Pb3–O1	2.680(9)
Pb1–O6	2.820(8)	Pb2–OH9	2.711(8)	Pb3–O1	2.717(9)
Pb1–O4	2.929(10)	Pb2–O1	2.851(11)	Pb3–O3	2.929(13)
Pb1–O1	3.094(11)	Pb2–O8	2.862(9)	Pb3–O2	3.188(12)
Pb1–O3	3.193(12)	Pb2–O2	2.945(10)	Pb3–O4	3.222(9)
Pb1–O2	3.315(11)	<Pb–O>	2.684	<Pb–O>	2.763
<Pb–O>	2.805				
C–O1	1.248(22)	Te–O4	1.896(10)	Cu–O7	1.942(9)
C–O2	1.304(18)	Te–O5	1.900(10)	Cu–O6	1.948(10)
C–O3	1.323(18)	Te–O6	1.921(10)	Cu–O8	1.952(9)
<C–O>	1.292	Te–O7	1.933(8)	Cu–O4	1.972(10)
		Te–O8	1.942(9)	Cu–O5	2.527(11)
OH9···O3	2.875(15)	Te–OH9	1.994(9)	<Cu–O>	2.068
OH10···O5	2.823(14)	<Te–O>	1.931		

Table 7. Bond valence sums for agaite. Values are expressed in valence units.

	O1	O2	O3	O4	O5	O6	O7	O8	OH9	OH10	Σ
C	1.468	1.262	1.199								3.929
Te				1.058	1.047	0.958	0.989	0.935	0.812		5.799
Cu				0.453	0.101	0.483	0.491	0.478			2.007
Pb1	0.099	0.063	0.081	0.189 0.139		0.174	0.541	0.476		0.322	2.084
Pb2	0.163	0.135			0.292 0.278	0.396		0.160	0.217	0.314	1.951
Pb3	0.231 0.215	0.290 0.082	0.291 0.139	0.077						0.582	1.907
H9			0.167						0.833		1.000
H10					0.173					0.827	1.000
Σ	2.176	1.832	1.877	1.916	1.891	2.011	2.021	2.049	1.862	2.045	

Notes: Pb^{2+}–O bond strengths from Krivovichev and Brown (2001); C^{4+}–O, Te^{6+}–O and Cu^{2+}–O bond strengths from Brown and Altermatt (1985); hydrogen-bond strengths based on O···O bond lengths, also from Brown and Altermatt (1985).

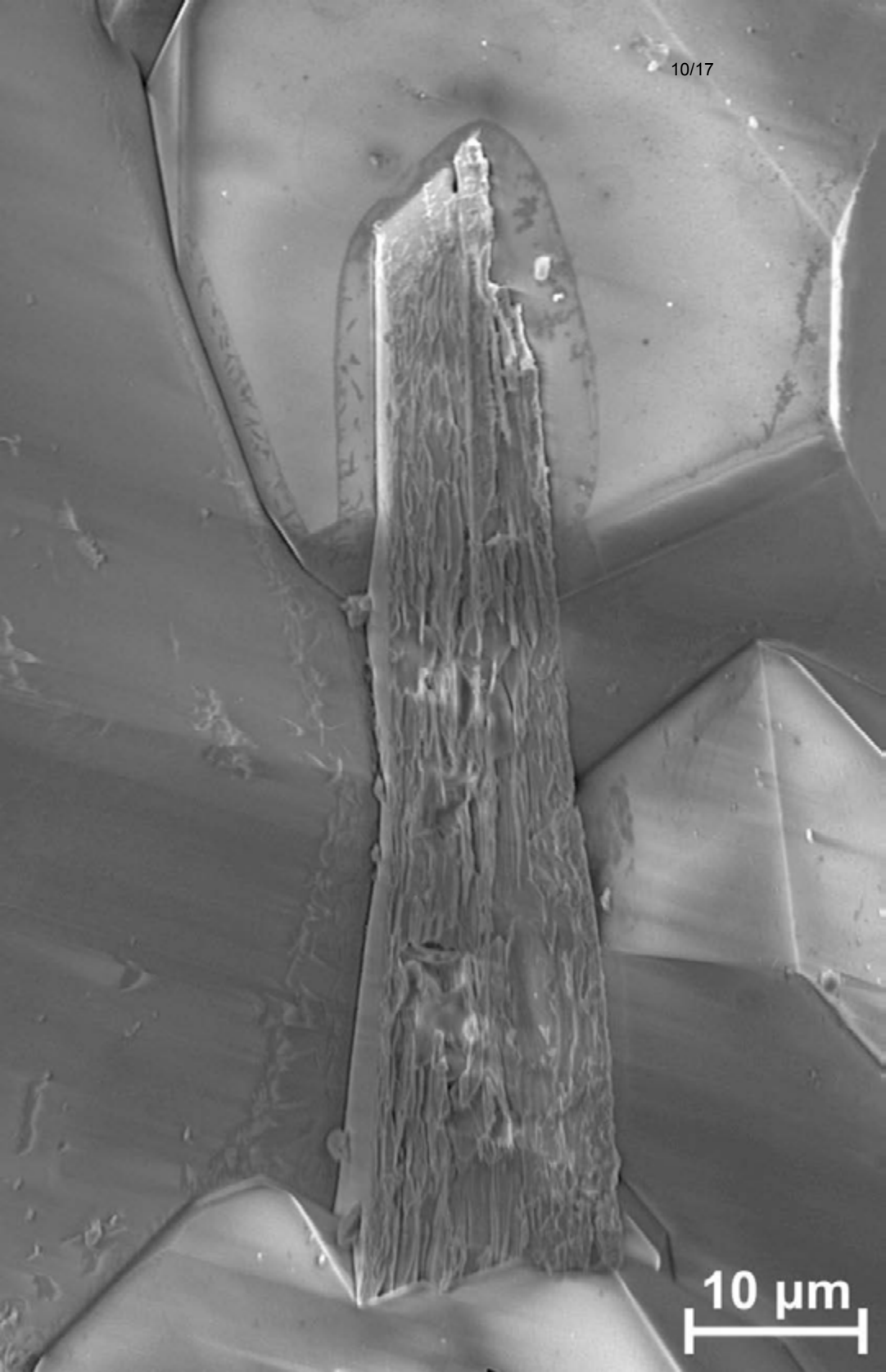
10 µm

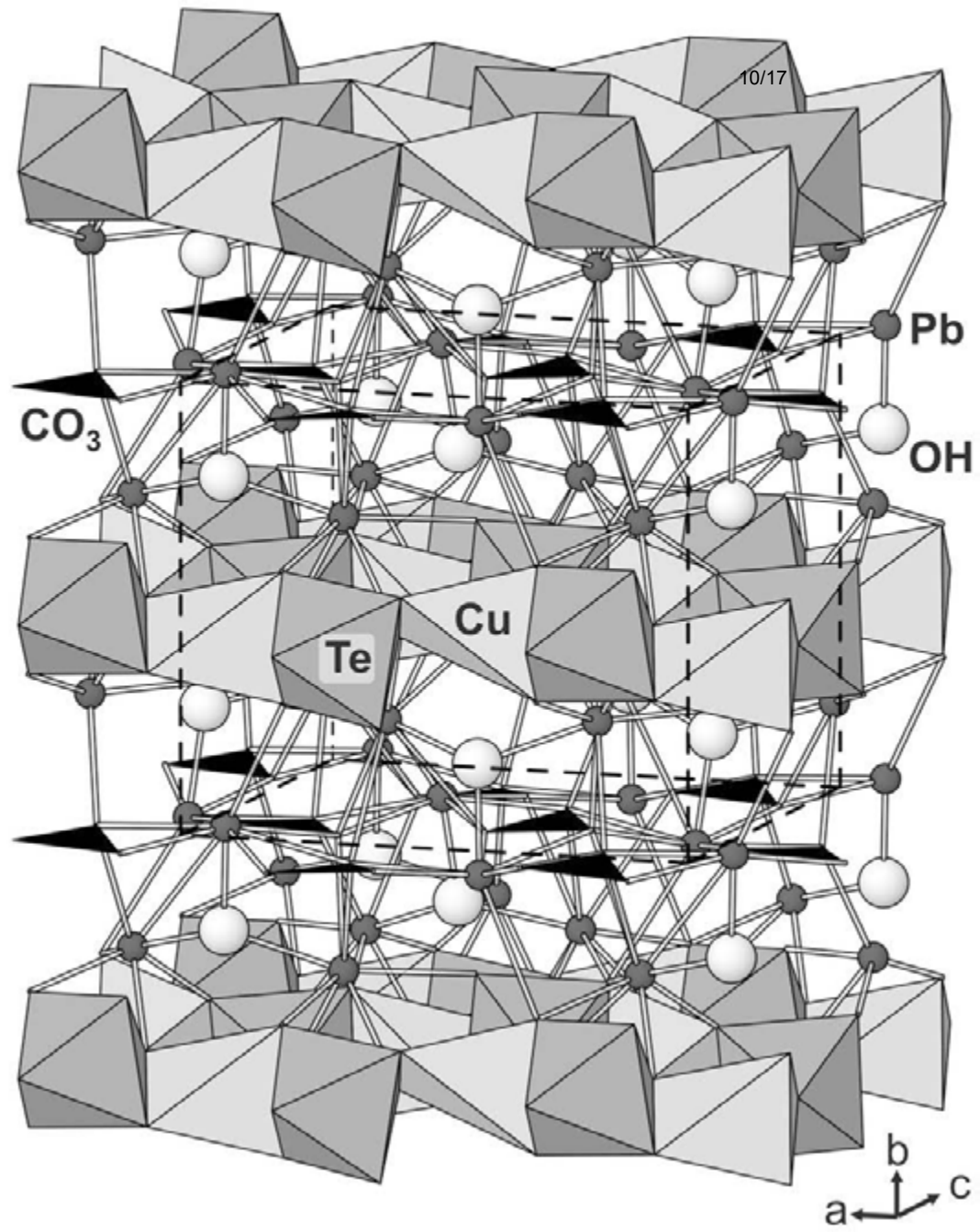
Pb
CO_3
OH
Cu
Te
b
c
a

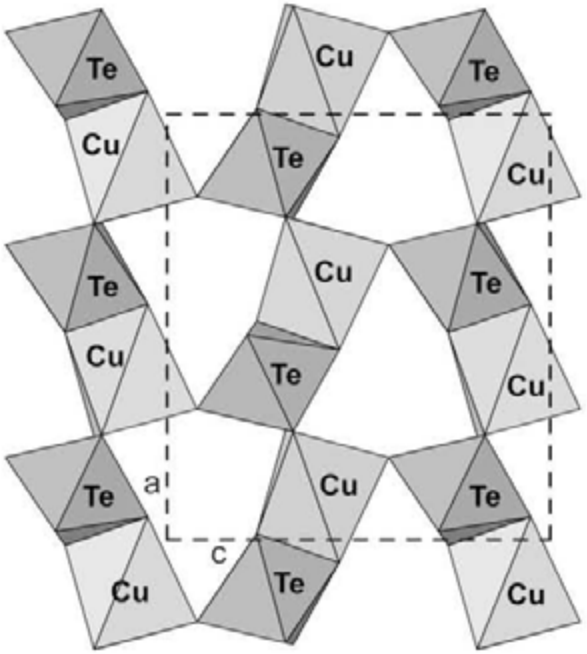

agaite

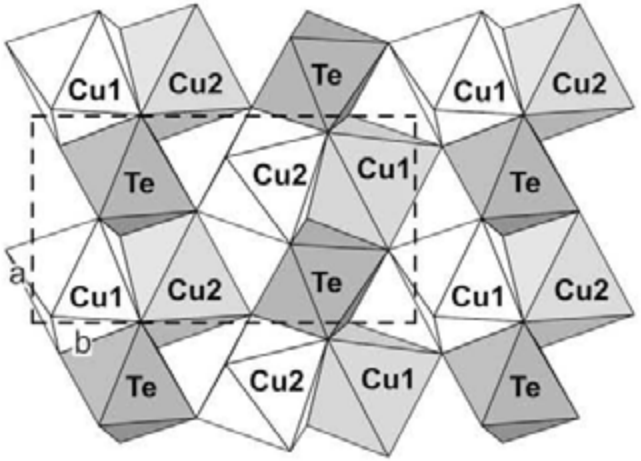

timroseite

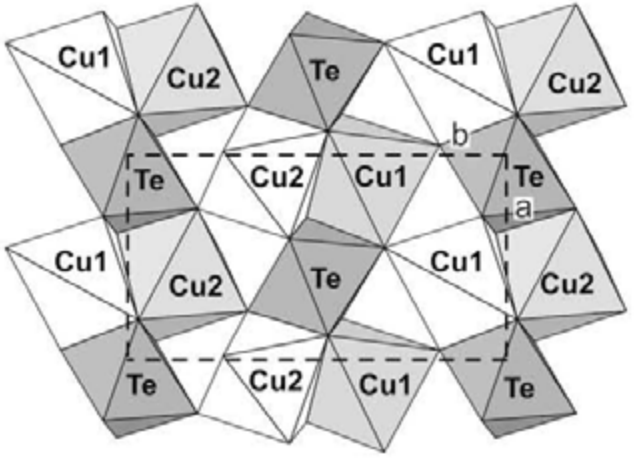

paratimroseite

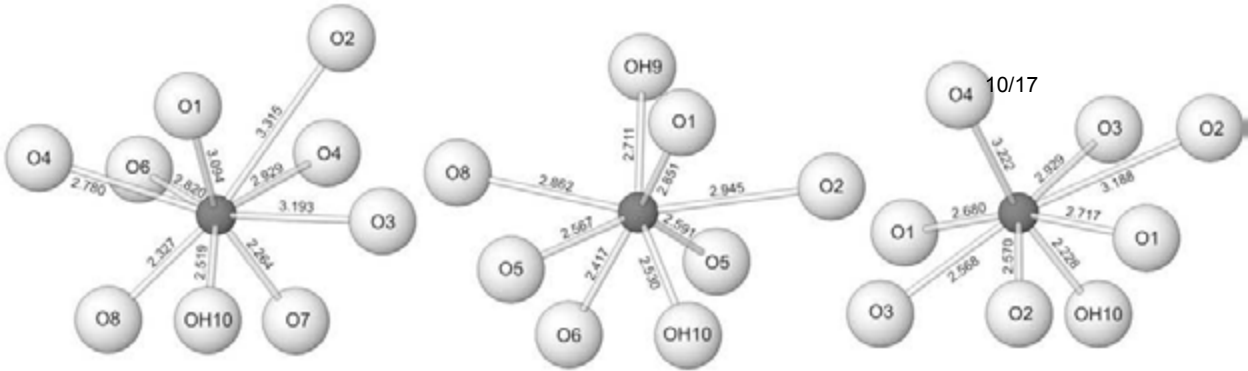
O2
O1
3.315
O4
O6
3.094
2.820
2.929
O4
2.780
3.193
O3
2.327
2.519
2.264
O8
OH10
O7
Pb1
OH9
O1
2.711
2.851
O8
2.862
2.945
O2
2.567
2.591
O5
O5
2.417
2.526
O6
OH10
Pb2
O4
10/17
3.222
2.929
O3
O2
3.188
2.680
2.717
O1
O1
2.568
2.579
2.228
O3
O2
OH10
Pb3